Sigma-Bond Metathesis Reactions of Zirconocene Alkyl Cations with Phenylsilane

Fan Wu and Richard F. Jordan*

Department of Chemistry, The University of Chicago, 5735 South Ellis Avenue, Chicago, Illinois 60637

Received November 20, 2004

The zirconocene methyl cations $[(C_5R_5)_2ZrMe(ClC_6D_5)][B(C_6F_5)_4]$ (C_5R_5 = C_5H_5 (**1a**), C_5H_4Me (**1b**)) react with $PhSiH_3$ in the dark to yield $[\{(C_5R_5)_2Zr(\mu\text{-}H)\}_2][B(C_6F_5)_4]_2$ (**5a**,**b**) and a mixture of $Ph_xMe_yH_zSi$ products. The reaction proceeds by initial Zr−C/Si−H σ-bond metathesis via a four-center transition state in which Si is β to Zr. In the presence of light, significant amounts of $[\{(C_5R_5)_2Zr(\mu\text{-}Cl)\}_2][B(C_6F_5)_4]_2$ (**4a**,**b**) are formed by photochemical reaction of $(C_5R_5)_2ZrH^+$ species with the chlorobenzene solvent. The azazirconacycle [*rac*-(EBI)Zr{η^2(*C*,*N*)-CH_2CHMe(6-phenyl-2-pyridyl)}][$B(C_6F_5)_4$] (**2**, EBI = 1,2-ethylene-bis-indenyl) does not react with $PhSiH_3$ at 23 °C. However at 85 °C, **2** deinserts propene to afford the η^2-pyridyl complex [*rac*-(EBI)Zr{η^2(*C*,*N*)-(6-phenyl-2-pyridyl)}][$B(C_6F_5)_4$] (**6**), which is catalytically isomerized to [*rac*-(EBI)Zr{η^2(*C*,*N*)-2-(2-pyridyl)phenyl}][$B(C_6F_5)_4$] (**7**) by $PhSiH_3$. The key step in this process is Zr−C/Si−H σ-bond metathesis of **6** with $PhSiH_3$ via a transition state in which Si is α to Zr. The less crowded azazirconacycle [Cp_2Zr\{η^2(*C*,*N*)-CH_2CHMe-(6-methyl-2-pyridyl)}][$B(C_6F_5)_4$] (**3**) reacts with $PhSiH_3$ directly to afford $[\{Cp_2Zr(SiPhH_2)\}_2]$-$[B(C_6F_5)_4]_2$ (**8**) via a transition state in which Si is α to Zr. Steric factors may play a role in determining the selectivity of these reactions.

Introduction

The development of productive catalytic C−H activation processes based on σ-bond metathesis reactions is an attractive goal.[1] Earlier we reported that $(C_5R_5)_2ZrR'^+$ species catalyze the net insertion of olefins into the ortho C−H bonds of 2-substituted pyridines in the presence of H_2 via the mechanism shown in Scheme 1.[2] However, as the key metallacycle cleavage step (step i) in Scheme 1 occurs by Zr−C bond hydrogenolysis, the C−Zr bond of the metallacycle is converted into a C−H bond in the disubstituted pyridine product with attendant loss of functionality. Therefore, alternative metallacycle cleavage reactions that install a functional group in the product are desirable.

One possible alternative metallacycle cleavage reaction is σ-bond metathesis with a silane, which could be incorporated into the hypothetical catalytic cycle in Scheme 2.

Scheme 1

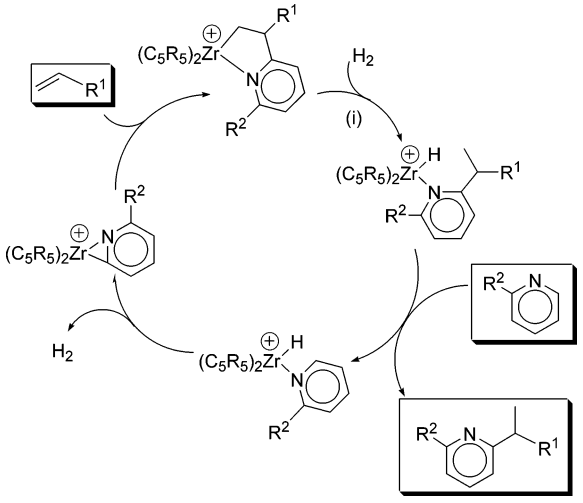

Several stoichiometric reactions of cationic (or cationic-like) group 4 metallocene alkyl or aryl species with $PhSiH_3$ have been reported. Tilley showed that CpCp*HfMe(μ-Me)$B(C_6F_5)_3$ (Cp = C_5H_5; Cp* = C_5Me_5) undergoes σ-bond metathesis with $PhSiH_3$ to afford CpCp*HfH(μ-H)$B(C_6F_5)_3$ and $PhMe_2SiH$.[3] Harrod reported that an in-situ generated "Cp_2ZrBu^+" species reacts with $PhSiH_3$ to afford a Cp_2ZrH^+ species.[4] Additionally, $PhSiH_3$ functions as a "silanolytic" chain transfer agent in olefin polymerization reactions catalyzed by $\{Me_2Si(C_5Me_4)N^tBu\}TiMe^+$, titanocene, and

* To whom correspondence should be addressed. E-mail: rfjordan@uchicago.edu.

(1) (a) Davies, J. A.; Watson, P. L.; Liebman, J. F.; Greenberg, A. *Selective Hydrocarbon Activation*; VCH: New York, 1990. (b) Pittard, K. A.; Lee, J. P.; Cundari, T. R.; Gunnoe, T. B.; Peterson, J. L. *Organometallics* **2004**, *23*, 5514. (c) Sadow, A. D., Tilley, T. D. *J. Am. Chem. Soc.* **2003**, *125*, 7971. (d) Sadow, A. D., Tilley, T. D. *Angew. Chem., Int. Ed.* **2003**, *42*, 803. (e) Labinger, J. A.; Bercaw, J. E. *Nature* **2002**, *417*, 507. (f) Shilov, A. E.; Shul'pin, G. B. *Chem. Rev.* **1997**, *97*, 2879. (g) Thompson, M. E. *J. Am. Chem. Soc.* **1987**, *109*, 203. (h) Watson, P. L. *J. Am. Chem. Soc.* **1983**, *105*, 6491.

(2) (a) Dagorne, S.; Rodewald, S.; Jordan, R. F. *Organometallics* **1997**, *16*, 5541. (b) Rodewald, S.; Jordan, R. F. *J. Am. Chem. Soc.* **1994**, *116*, 4491. (c) Guram, A. S.; Jordan, R. F.; Tayler, D. F. *J. Am. Chem. Soc.* **1991**, *113*, 1833. (d) Guram, A. S.; Jordan, R. F. *Organometallics* **1991**, *10*, 3470. (e) Guram, A. S.; Jordan, R. F. *Organometallics* **1990**, *9*, 2190. (f) Jordan, R. F.; Guram, A. S. *Organometallics* **1990**, *9*, 2116. (g) Jordan, R. F.; Taylor, D. F.; Baenziger, N. C. *Organometallics* **1990**, *9*, 1546. (h) Jordan, R. F.; Tayler, D. F. *J. Am. Chem. Soc.* **1989**, *111*, 778.

(3) (a) Sadow, A. D.; Tilley, T. D. *Organometallics* **2003**, *22*, 3577. (b) Sadow, A. D.; Tilley, T. D. *Organometallics* **2001**, *20*, 4457. (c) Sadow, A. D., Tilley, T. D. *J. Am. Chem. Soc.* **2003**, *125*, 9462. (d) $(C_5R_5)_2ZrMe^+$ species also catalyze the dehydropolymerization of $PhSiH_3$. See Toru, I.; Tilley, T. D. *Polyhedron* **1994**, *13*, 2231.

10.1021/om049099z CCC: $30.25
Publication on Web 04/28/2005

Scheme 2

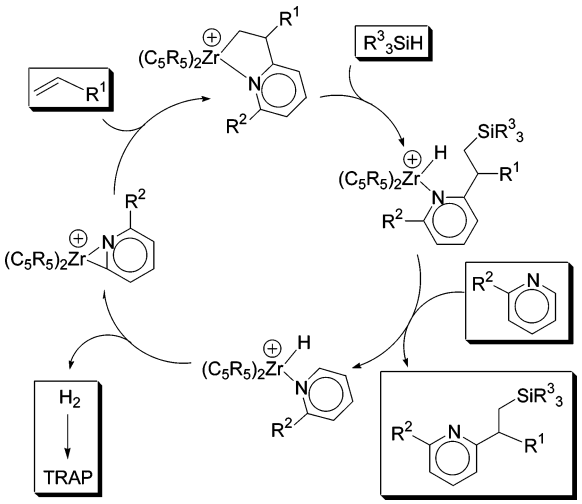

lanthanocene catalysts, and (less efficiently) Cp_2ZrR^+ catalysts, via reaction with active L_nM(polymeryl) species to produce L_nMH and polymeryl-$SiPhH_2$.[5] In all of these reactions, Si occupies the position that is β to the metal in the four-center σ-bond metathesis transition state **A** in eq 1.[6] An analogous transition state would be required in Scheme 2.

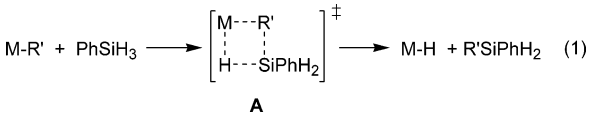

However, the opposite selectivity (i.e., Si α to the metal) has been observed in other cases.[7] For example, in-situ generated Cp'_2ZrH^+ ($Cp' = C_5H_4Me$) reacts with $PhSiH_3$ to afford the zirconocene silyl cation $Cp'_2Zr(SiH_2Ph)^+$, which adopts an interesting dinuclear structure.[4] In addition, as shown in Scheme 3, CpCp*HfH(μ-H)$B(C_6F_5)_3$ reacts with $PhSiH_3$ via competitive Si−H bond activation (transition state **B**) and Si−Ph bond activation (transition state **C**).[3b] Transition state **B** affords H_2 and CpCp*Hf$(SiPhH_2)^+$, which catalyzes silane dehydrocoupling reactions. Transition state **C**

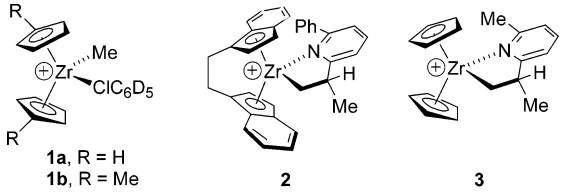

Figure 1. Zirconocene alkyl cations studied in this work. The counterion is $B(C_6F_5)_4^-$ in all cases.

Scheme 3

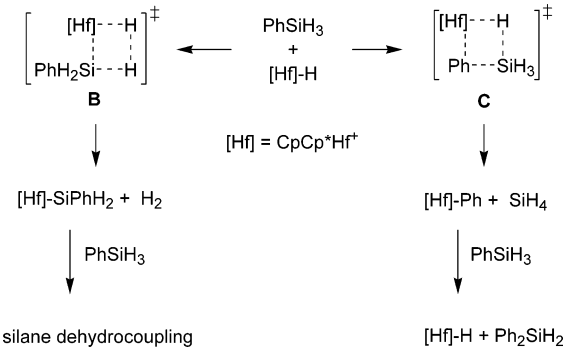

affords SiH_4 and CpCp*HfPh$^+$, which reacts further with $PhSiH_3$ to generate Ph_2SiH_2 and CpCp*HfH$^+$.

To probe the feasibility of exploiting "silanolytic" Zr−C bond cleavage reactions in olefin/pyridine coupling processes, we have studied the stoichiometric reactions of $PhSiH_3$ with several representative $(C_5R_5)_2ZrR'^+$ complexes.

Results

Synthesis of $(C_5R_5)_2ZrR'^+$ Species. Four $(C_5R_5)_2ZrR'^+$ species were studied in this work: the simple methyl complexes $[(C_5R_5)_2ZrMe(ClC_6D_5)][B(C_6F_5)_4]$ (C_5R_5 = Cp (**1a**), C_5R_5 = Cp′ (**1b**)) and the azazirconacycles [*rac*-(EBI)Zr{η^2(*C*,*N*)-CH_2CHMe(6-phenyl-2-pyridyl)}][$B(C_6F_5)_4$] (**2**, EBI = 1,2-ethylene-bis-indenyl) and [$Cp_2Zr\{\eta^2(C,N)$-CH_2CHMe(6-methyl-2-pyridyl)}][$B(C_6F_5)_4$] (**3**). These species are shown in Figure 1.

Complexes **1a**,**b** were generated in C_6D_5Cl solution by the reaction of the corresponding zirconocene dimethyl complexes with $[Ph_3C][B(C_6F_5)_4]$ as shown in eq 2 and described in detail elsewhere.[8]

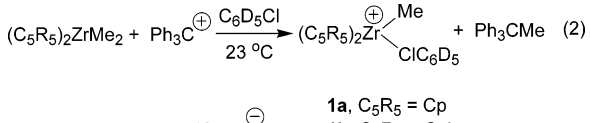

Complexes **2** and **3** were prepared by the reaction of the corresponding in-situ generated $(C_5R_5)_2Zr(\eta^2$-pyrid-2-yl)$^+$ species with propene, as shown in Scheme 4 and described earlier for the corresponding $MeB(C_6F_5)_3^-$ and BPh_4^- salts.[2a,h]

Reaction of $[Cp_2ZrMe(ClC_6D_5)][B(C_6F_5)_4]$ (1a) with $PhSiH_3$. The reaction of **1a** and 1 equiv of $PhSiH_3$ under ambient room light in C_6D_5Cl for 20 min at 23 °C results in complete consumption of the two reactants and formation of a red oil.[9] The oil gradually solidifies over the course of several days. The resulting orange solid is insoluble in hydrocarbon and chlorinated sol-

(4) (a) Dioumaev, V. K.; Harrod, J. F. *Organometallics* **1997**, *16*, 2798. (b) Dioumaev, V. K.; Harrod, J. F. *Organometallics* **1996**, *15*, 3859. (c) Dioumaev, V. K.; Harrod, J. F. *Organometallics* **1994**, *13*, 1548.

(5) (a) Makio, H.; Koo, K.; Marks, T. J. *Macromolecules* **2001**, *34*, 4676. (b) Koo, K.; Marks, T. J. *J. Am. Chem. Soc.* **1999**, *121*, 8791. (c) Koo, K.; Marks, T. J. *J. Am. Chem. Soc.* **1998**, *120*, 4019. (d) Fu, P.; Marks, T. J. *J. Am. Chem. Soc.* **1995**, *117*, 10747.

(6) For other σ-bond metathesis reactions of Zr and f-element metal alkyl complexes with silanes that proceed via four-center transition states in which Si is β to the metal, see: (a) Voskoboynikov, A. Z.; Parshina, I. N.; Shestakova, A. K.; Butin, K. P.; Beletskaya, I. P.; Kuz'mina, L. G.; Howard, J. A. K. *Organometallics* **1997**, *16*, 4041. (b) Dash, A. K.; Gourevich, I.; Wang, J. Q.; Wang, J.; Kapon, M.; Eisen, M. S. *Organometallics* **2001**, *20*, 5084. (c) Molander, G. A.; Julis, M. *J. Am. Chem. Soc.* **1995**, *117*, 4415. (d) Gountchev, T. I.; Tilley, T. D. *Organometallics* **1999**, *18*, 5661. (e) Fu, P.; Brard, L.; Li, Y.; Marks, T. J. *J. Am. Chem. Soc.* **1995**, *117*, 7157. (f) de Haan, K. H.; Wielstraand, Y.; Eshuis, J. J. W.; Teuben, J. H. *J. Organomet. Chem.* **1987**, *323*, 181. (g) Molander, G. A.; Corrette, C. P. *Tetrahedron Lett.* **1998**, *39*, 5011.

(7) For σ-bond metathesis reactions of group 3 and lanthanide metal alkyl complexes with silanes that proceed via four-center transition states in which Si is α to the metal, see ref 1d and: (a) Radu, N. S.; Tilley, T. D.; Rheingold, A. L. *J. Organomet. Chem.* **1996**, *516*, 41. (b) de Haan, K. H.; de Boer, J. L.; Teuben, J. H. *Organometallics* **1986**, *5*, 1726.

(8) Wu, F.; Dash, A. K.; Jordan, R. F. *J. Am. Chem. Soc.* **2004**, *126*, 15360.

Scheme 4

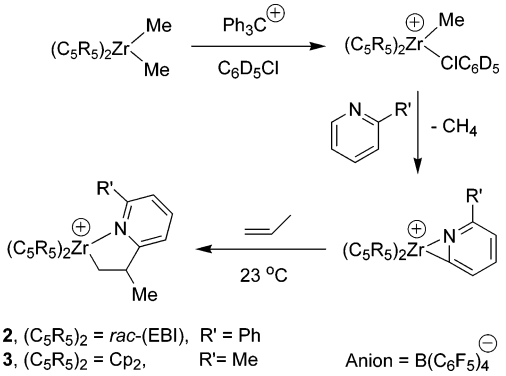

vents, but is soluble in THF and CH_3CN. The ^1H NMR spectrum of a THF-d_8 solution of the solid (isolated after 6 days), prepared and maintained at −90 °C, shows that two dinuclear dicationic complexes, $[\{Cp_2Zr(\mu\text{-}Cl)\}_2][B(C_6F_5)_4]_2$ (**4a**) and $[\{Cp_2Zr(\mu\text{-}H)\}_2][B(C_6F_5)_4]_2$ (**5a**), are present in a 1:3 ratio (total > 90%). These species were identified by independent synthesis (vide infra). Additionally, single crystals of **4a** were obtained from the solid and identified by X-ray diffraction. A mixture of silanes is formed, including $PhSiMeH_2$, $PhSiMe_2H$, $PhSiMe_3$, Ph_2SiH_2, Ph_2SiMeH, Ph_2SiMe_2, Ph_3SiH, Ph_3SiMe, and Ph_4Si, which were identified by GC-MS analysis of the reaction mixture. No disilanes or higher polysilanes were observed by GC-MS.[3d]

In a series of similar experiments under ambient room light, the organometallic products were analyzed at different stages of the oil solidification process. These analyses revealed that the ratio of **4a/5a** increases with time. For example, the oil isolated after a 20 min reaction time comprises a 1:12 mixture of **4a** and **5a**. This ratio increases with time to 1:9 (10 h), 1:5 (20 h), and 1:4 (40 h), and finally levels off at 1:3 after 6 days, at which point the oil is completely solidified. In contrast, the reaction of **1a** with $PhSiH_3$ under the same conditions, but protected from light, affords **5a** in greater than 90% yield without formation of **4a**. These observations imply that **4a** is formed from **5a** or the corresponding mononuclear species Cp_2ZrH^+ or $Cp_2ZrH(ClC_6D_5)^+$ by a photochemical process. The overall reaction between **1a** and 1 equiv of $PhSiH_3$ is shown in Scheme 5.

Independent Synthesis of $[\{Cp_2Zr(\mu\text{-}Cl)\}_2][B(C_6F_5)_4]_2$ (4a). Complex **4a** can be generated by two routes (eq 3). The reaction of **1a** with Ph_3CCl in C_6D_5Cl affords orange crystalline **4a** in 90% yield. Alternatively, the reaction of **1a** with Me_3SiCl in C_6D_5Cl affords analytically pure **4a** in 80% yield.

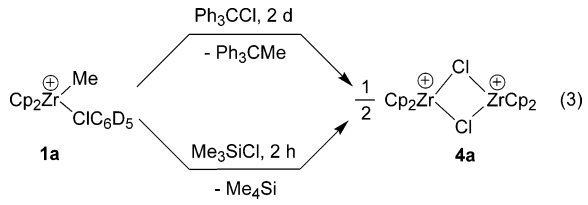

The solid state structure of **4a** contains $\{Cp_2Zr(\mu\text{-}Cl)\}_2^{2+}$ and $B(C_6F_5)_4^-$ ions, with no close interionic contacts. The dinuclear dication of **4a** is shown in Figure 2 and comprises two bent zirconocene units linked by two bridging chloride ligands. The $Zr(\mu\text{-}Cl)_2Zr$ core is planar. The Zr−(μ-Cl) bonds (average 2.575(1) Å) are elongated compared to that in Cp_2ZrCl_2 (2.446(3) Å), as expected.[10]

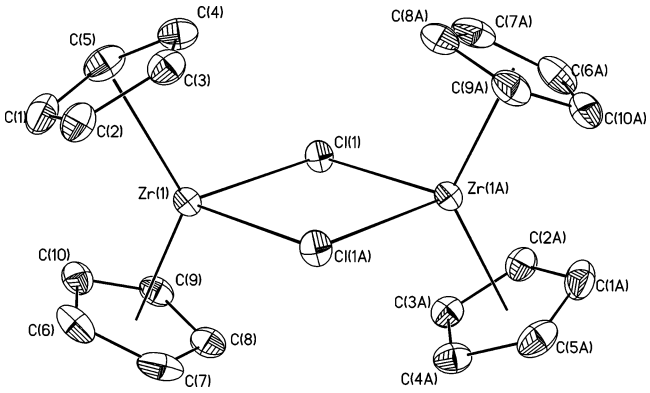

Figure 2. ORTEP view of the $\{Cp_2Zr(\mu\text{-}Cl)\}_2^{2+}$ dication of **4a**. Hydrogen atoms are omitted. Key bond distances (Å) and angles (deg): Zr(1)−Cl(1) 2.569(1); Zr(1)−Cl(1A) 2.581(1); Zr(1)−Centroid(1) 2.174(1); Zr(1)−Centroid(2) 2.164(1); Cl(1A)−Zr(1)−Cl(1) 82.0(1); Zr(1)−Cl(1)−Zr(1A) 98.0(1); Centroid(1)−Zr(1)−Centroid(2) 129.8(1).

Scheme 5

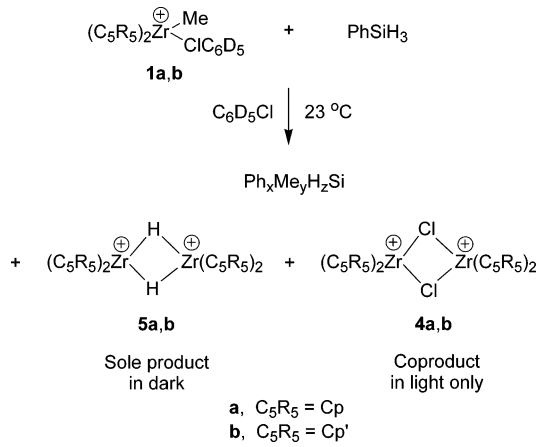

Scheme 6

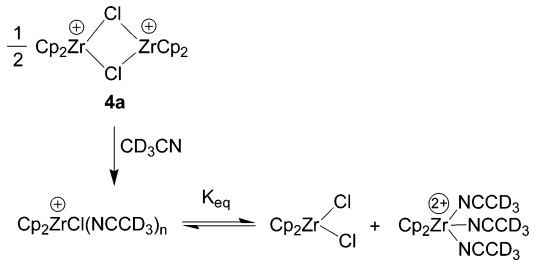

Complex **4a** dissolves in CD_3CN to form $Cp_2ZrCl(NCCD_3)_n^+$, which undergoes partial disproportionation to Cp_2ZrCl_2 and $Cp_2Zr(NCCD_3)_3^{2+}$, as shown in Scheme 6 and observed previously for the analogous BPh_4^- salt.[11] The ^1H NMR spectrum of the CD_3CN solution of **4a** consists of three resonances at δ 6.52, 6.51, and 6.39, which correspond to the Cp resonances of Cp_2ZrCl_2, Cp_2-

(9) In this paper, the phrase ambient room light refers to standard fluorescent room lighting.

(10) Prout, K.; Cameron, T. S.; Forder, R. A.; Critchley, S. R.; Denton, B.; Rees, G. V. *Acta Crystallogr.* **1974**, *B30*, 2290.

(11) Jordan, R. F.; Echols, S. F. *Inorg. Chem.* **1987**, *26*, 383.

Scheme 7

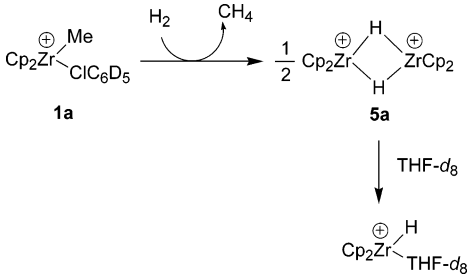

$Zr(NCCD_3)_3^{2+}$, and $Cp_2ZrCl(NCCD_3)_n^+$, respectively. The equilibrium constant, $K_{eq} = [Cp_2ZrCl_2][Cp_2Zr(NCCD_3)_3^{2+}][Cp_2ZrCl(NCCD_3)_n^+]^{-2}$, is 2.0(1) at 23 °C in CD_3CN. A similar value (K_{eq} = 1.0(1) at 23 °C) was observed for the BPh_4^- salt.[11] The ^{1}H NMR spectrum of **4a** in THF-d_8 comprises a singlet at δ 6.87.

The direct analogue of **4a**, $[\{Cp_2Zr(\mu\text{-Cl})\}_2][BF_4]_2$, was generated previously by the reaction of $\{Cp_2Zr(\mu\text{-Cl})\}_2$ with $AgBF_4$ and characterized by elemental analysis and conductivity.[12a] The bromide complexes $[\{1,2\text{-}(SiMe_2)_2(\eta^5\text{-}C_5H_3)_2Zr(\mu\text{-Br})\}_2][B(C_6F_5)_4]_2$[12b] and $[\{Cp_2Hf(\mu\text{-Br})\}_2][B(C_6F_5)_4]_2$[3c] were also reported.

Independent Synthesis of $[\{Cp_2Zr(\mu\text{-H})\}_2][B(C_6F_5)_4]_2$ (5a). The reaction of **1a** with 1 atm of H_2 in C_6D_5Cl in the absence of light (23 °C, Scheme 7) results in complete consumption of **1a** within 10 min and precipitation of **5a** as a yellow solid. **5a** is isolated as an analytically pure solid in 95% yield. However, the reaction of **1a** with H_2 under ambient room light affords a 25:1 mixture of **5a** and **4a**.

The IR spectrum of solid **5a** contains a ν_{Zr-H} band at 1337 cm^{-1}, which shifts to 1040 cm^{-1} in $[\{Cp_2Zr(\mu\text{-D})\}_2][B(C_6F_5)_4]_2$ (**5a**-d_2; prepared from **1a** and D_2). The ν_{Zr-H} value for **5a** is within the range observed for bridging hydrides in other d^0 metallocene systems, e.g., $\{Cp_2Zr(\mu\text{-H})(CH_2C_6H_{11})\}_2$ (1380 cm^{-1}), $\{Cp_2ZrH(\mu\text{-H})\}_2$ (1300 cm^{-1}), and $\{(C_5R_5)_2M(\mu\text{-H})(THF)\}_2$ (1240−1350 cm^{-1}; C_5R_5 = Cp or Cp′; M = Lu, Er, Y).[13] Higher ν_{Zr-H} values were observed for the terminal hydrides $Cp_2ZrH(THF)^+$ (1450 cm^{-1}), $Cp_2ZrH(PMe_3)_2^+$ (1498 cm^{-1}), and $Cp'_2ZrH(THF)^+$ (1390 cm^{-1}).[14] On the basis of these results, **5a** is assigned a dimeric dicationic structure analogous to that of **4a**.

The ^{1}H NMR spectrum of a solution of **5a** in THF-d_8 prepared and maintained at −90 °C displays a Cp resonance at δ 6.75 and a hydride resonance at δ −0.53, which is consistent with a dinuclear μ-H structure. When the solution is warmed to 23 °C, the Cp and hydride resonances shift to δ 6.20 and 5.78 respectively, indicating that THF-d_8 converts the dimeric structure to a monomeric terminal hydride species $Cp_2ZrH(THF\text{-}d_8)^+$ (Scheme 7).[15] The ^{1}H NMR resonances of bridging hydrides are generally upfield of terminal hydride resonances in d^0 zirconocene systems (e.g., $\{Cp'_2ZrH(\mu\text{-H})\}_2$ (δ_{Zr-H} 3.75; $\delta_{\mu-H}$ −2.98),[13c] {(tetrahydroindenyl)$_2$-$ZrH(\mu\text{-H})\}_2$ (δ_{Zr-H} 4.59; $\delta_{\mu-H}$ −1.56),[13b] $Cp'_2ZrH(THF)^+$ (δ 5.88),[14a] $(C_5Me_5)_2ZrH_2$ (δ 7.46),[13g] $(C_5Me_5)_2ZrH(OMe)$ (δ 5.70)[13g]). THF solutions of **5a** solidify within 1 h at 23 °C due to polymerization of the solvent by **5a**, as described earlier for $Cp'_2ZrH(THF)^+$.[14a]

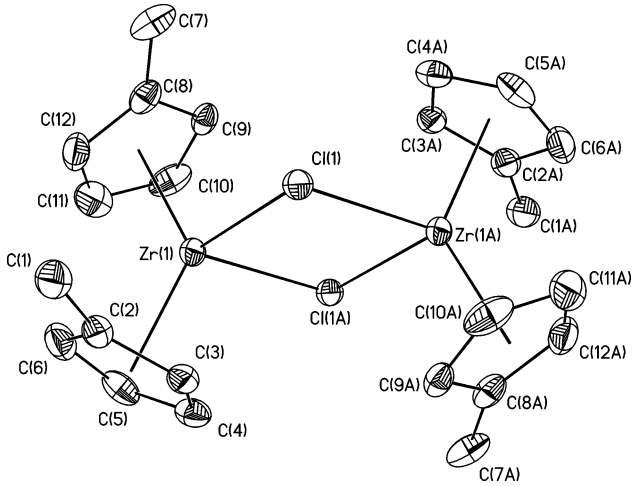

Figure 3. ORTEP view of the $\{Cp'_2Zr(\mu\text{-Cl})\}_2^{2+}$ dication of **4b**. Hydrogen atoms are omitted. Key bond distances (Å) and angles (deg): Zr(1)−Cl(1) 2.577(5); Zr(1)−Cl(1A) 2.588(5); Zr(1)−Centroid(1) 2.159(5); Zr(1)−Centroid(2) 2.177(5); Cl(1A)−Zr(1)−Cl(1) 84.2(1); Zr(1)−Cl(1)−Zr(1A) 95.8(1); Centroid(1)−Zr(1)−Centroid(2) 130.0(1).

Reaction of $[Cp'_2ZrMe(ClC_6D_5)][B(C_6F_5)_4]$ (1b) with $PhSiH_3$. Complex **1b** reacts with $PhSiH_3$ under ambient room light in a fashion similar to **1a** to yield $[\{Cp'_2Zr(\mu\text{-Cl})\}_2][B(C_6F_5)_4]_2$ (**4b**) and $[\{Cp'_2Zr(\mu\text{-H})\}_2][B(C_6F_5)_4]_2$ (**5b**) in a 1:2 ratio as the major organometallic products, as shown in Scheme 5. Only **5b** is formed when the reaction is conducted in the absence of light. In addition, the same series of silane products as formed in the reaction of **1a** is produced. The identities of **4b** and **5b** were confirmed by independent synthesis, and the structure of **4b** was confirmed by X-ray diffraction (Figure 3).

Proposed Mechanism for the Reaction of 1a,b with $PhSiH_3$. The key observations that are relevant to the mechanism of the reaction of **1a**,**b** with $PhSiH_3$ in Scheme 5 are as follows: (i) Only a trace amount of CH_4 is formed; (ii) the exclusive Zr product in the dark reaction is Zr-hydride species **5a**,**b**; and (iii) the Zr-Me group of **1a**,**b** ends up in the $Ph_xMe_yH_zSi$ ($x + y + z$ = 4) silane mixture. These observations are consistent with the σ-bond metathesis process in Scheme 8, in which Si occupies the position β to Zr in transition state **D**. The initially formed $(C_5R_5)_2ZrH^+$ species **E** (which may be solvated) is trapped as dimer **5a**,**b** in the dark reaction. In the presence of light, **E** and/or **5a**,**b** undergo competitive photochemical reaction with the chlorobenzene solvent to yield **4a**,**b**.[16,17]

(12) (a) Cuenca, T.; Royo, P. *J. Organomet. Chem.* **1985**, *293*, 61. (b) Brandow, C. G.; Mendiratta, A.; Bercaw, J. E. *Organometallics* **2001**, *20*, 4253. For other d^0 $\{L_nM(\mu\text{-X})\}_2^{2+}$ species see: (c) Gomez, R.; Green, M. L. H.; Haggitt, J. L. *J. Chem. Soc., Dalton Trans.* **1996**, 936. (d) Zhang, Y.; Reeder, E. K.; Keaton, R. J.; Sita, L. R. *Organometallics* **2004**, *23*, 3512. (e) Vollmerhaus, R.; Rahim, M.; Tomaszewski, R.; Xin, S.; Taylor, N. J.; Collins, S. *Organometallics* **2000**, *19*, 2161.

(13) (a) Gell, K. I.; Posin, B.; Schwartz, J.; Williams, G. M. *J. Am. Chem. Soc.* **1982**, *104*, 1846. (b) Weigold, H.; Bell, A. P.; Willing, R. I. *J. Organomet. Chem.* **1974**, *73*, C23. (c) Jones, S. B.; Peterson, J. L. *Inorg. Chem.* **1981**, *20*, 2889. (d) Wailes, P. C.; Weigold, H. *J. Organomet. Chem.* **1970**, *24*, 405. (e) James. B. D.; Nanda, R. K.; Wallbridge, M. G. H. *Inorg. Chem.* **1967**, *6*, 1979. (f) Evans, W. J.; Meadows, J. H.; Wayda, A. L.; Hunter, W. J.; Atwood, J. L. *J. Am. Chem. Soc.* **1982**, *104*, 2008. (g) Manriquez, J. M.; MaAlister, D. R.; Sanner, R. D.; Bercaw, J. E. *J. Am. Chem. Soc.* **1976**, *98*, 6733.

(14) (a) Guo, Z.; Bradley, P. K.; Jordan, R. F. *Organometallics* **1992**, *11*, 2690. (b) Jordan, R. F.; Bajgur, C. S.; Dasher, W. E. *Organometallics* **1987**, *6*, 1041.

(15) The analogous BPh_4^- salt is insoluble. See ref 14a.

Scheme 8

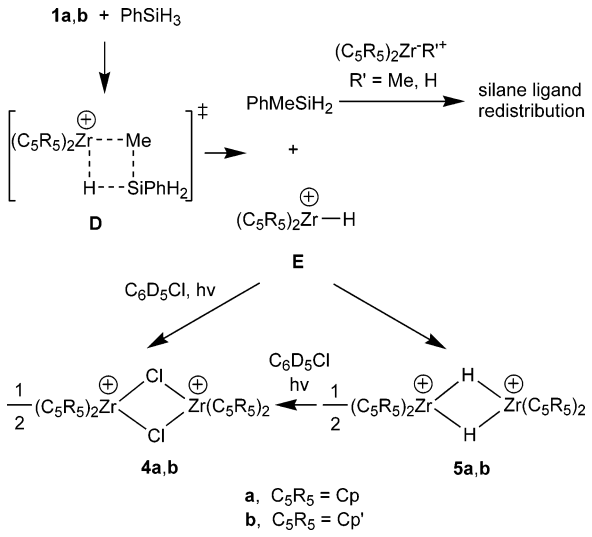

Scheme 9

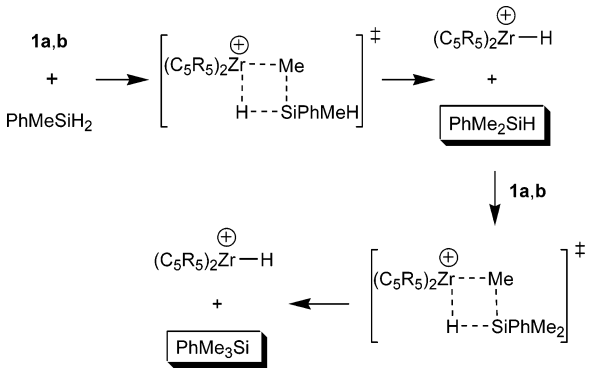

The silane products can form by two pathways. First, σ-bond metathesis of the Zr−Me bond of **1a**,**b** with the Si−H bond of $PhMe_xH_{3-x}Si$ (x = 1, 2) will produce $PhMe_{x+1}H_{2-x}Si$, as shown in Scheme 9.

The formation of diphenyl silanes, triphenyl silanes, and Ph_4Si requires redistribution of Si−Ph groups. As suggested in Scheme 10, the key step in this process is probably σ-bond metathesis of the Si−Ph bond of $PhSiH_3$ (or other Ph−Si species) and the Zr−H bond of the initially formed $(C_5R_5)_2ZrH^+$ species to produce $(C_5R_5)_2ZrPh^+$ and SiH_4. Subsequent reaction of $(C_5R_5)_2ZrPh^+$ with $Ph_xMe_yH_zSi$ ($x + y + z = 4$) should produce $Ph_{x+1}Me_yH_{z-1}Si$ with regeneration of $(C_5R_5)_2ZrH^+$ (cf. $(C_5R_5)_2ZrMe^+$ reactions in Scheme 8). Consistent with this proposal, the ^{1}H NMR of spectrum of a THF-d_8 solution of the oil formed in the reaction of **1a** with

Scheme 10

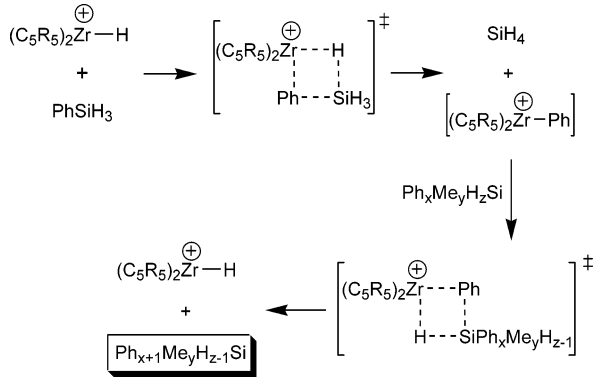

Scheme 11

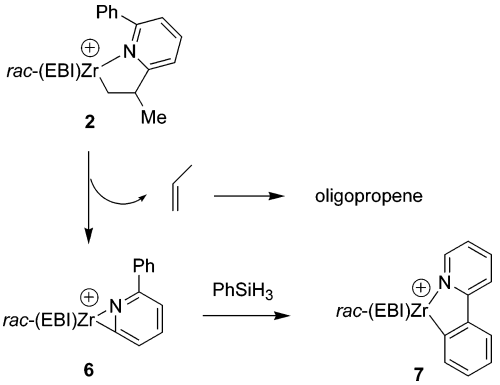

$PhSiH_3$ (20 min, in the light) contains resonances for $Cp_2ZrH(THF\text{-}d_8)^+$ (88%), $Cp_2ZrCl(THF\text{-}d_8)^+$ (8%), $Cp_2ZrPh(THF\text{-}d_8)^+$ (2%),[18] and several other minor Cp_2Zr species. This oil reacts with $PhSiH_3$ to afford Ph_2SiH_2, Ph_3SiH, Ph_4Si, and SiH_4. Also, as noted above, Tilley showed that CpCp*HfH(μ-H)B(C_6F_5)$_3$ mediates redistribution of $PhSiH_3$ to Ph_2SiH_2 and SiH_4.[3b,19−22]

Reaction of [*rac*-(EBI)Zr{η^2(*C*,*N*)-CH$_2$CHMe(6-phenyl-2-pyridyl)}][B(C_6F_5)$_4$] (2) and $PhSiH_3$. Complex **2** does not react with 2.5 equiv of $PhSiH_3$ at 23 °C in C_6D_5Cl. However, heating the mixture to 85 °C for 20 h results in complete consumption of **2** and consumption of 1.5 equiv of $PhSiH_3$. The major silane product is Ph_2SiH_2 (0.7 equiv vs Zr), and small amounts of Ph_3SiH, Ph_4Si, and SiH_4 are also formed. No other significant Si-containing products could be identified. ^{1}H NMR analysis of the reaction mixture shows that a C_1-symmetric Zr species, [*rac*-(EBI)Zr{η^2(*C*,*N*)-2-(2-pyridyl)phenyl}][B(C_6F_5)$_4$] (**7**, Scheme 11), is formed in 90% yield and that atactic oligopropene is also produced. These observations suggest that, at 85 °C, **2** undergoes deinsertion of propene to generate [*rac*-(EBI)Zr{η^2(*C*,*N*)-(6-phenyl-2-pyridyl)}][B(C_6F_5)$_4$] (**6**),[2a] which in turn reacts with $PhSiH_3$ to yield **7**, as shown in Scheme 11. **7** is an isomer of **6**. The cationic zirconocene species in the system catalyze the propene oligomerization and silane redistribution reactions. Independent experiments show that **6** reacts rapidly (<30 min) with $PhSiH_3$ at 23 °C to afford **7** in 90% yield. Ph_2SiH_2 is also formed in this reaction.

The ^{1}H NMR spectrum of **7** generated by the $PhSiH_3$ reaction in Scheme 11 is partially obscured by the

(16) **1a**,**b** also react photochemically with chlorobenzene to yield **4a**,**b** (see ref 8), but much more slowly (20% conversion after 8 days) than **4a**,**b** are formed in the $PhSiH_3$ reactions (20 min). The mechanism of these photochemical reactions is unknown at present. The reaction of **1a**,**b** with $PhSiH_3$ produces 1 equiv of C_6D_5H per $(C_5R_5)_2ZrCl^+$ unit of **4a**,**b**, which was identified by GC-MS and ^{1}H NMR. In addition, a trace amount of $C_6D_5-C_6D_5$ was detected by GC-MS. These observations suggest that homolytic cleavage of the Cl−C_6D_5 bonds of $(C_5R_5)_2ZrR(ClPh)^+$ species occurs.

(17) The −90 °C ^{1}H NMR spectrum of a THF-d_8 solution of the solid isolated from the reaction of **1a** with $PhSiH_3$ after 6 days, prepared and maintained at −90 °C, contains resonances for $Cp_2ZrH(THF\text{-}d_8)^+$, corresponding to 2% of the total Cp_2Zr species present, along with major resonances for **4a** and **5a**. The mononuclear hydride $Cp_2ZrH(THF\text{-}d_8)^+$ could form by trace solvolysis of dimer **5a** or by solvolysis of a mixed dinuclear hydride chloride species $\{Cp_2Zr\}_2(\mu\text{-H})(\mu\text{-Cl})^{2+}$. We conclude that, at most, only a trace quantity of this mixed species is present in the isolated solid.

(18) Borkowsky, S. L.; Jordan, R. F.; Hinch, G. D. *Organometallics* **1991**, *10*, 1268.

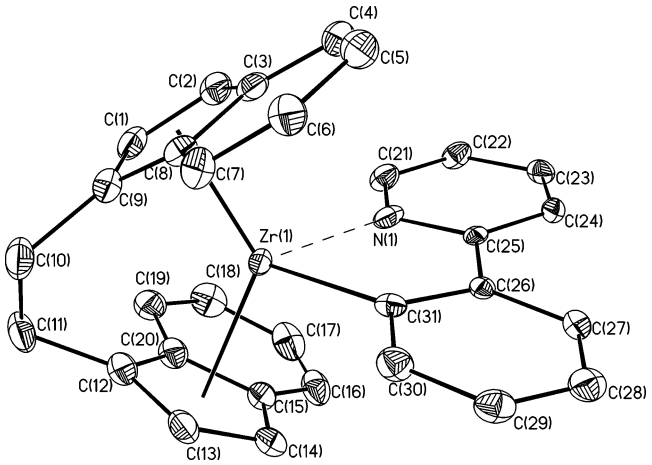

Figure 4. ORTEP view of the *rac*-(EBI)Zr{η^2(*C*,*N*)-2-(2-pyridyl)-phenyl}$^+$ cation of **7**. Hydrogen atoms are omitted. Key bond distances (Å) and angles (deg): Zr(1)−N(1) 2.260(6); Zr(1)−C(31) 2.254(6); Zr(1)−Centroid(1) 2.177(5); Zr(1)−Centroid(2) 2.196(5); Centroid(1)−Zr(1)−Centroid(2) 127.5(4); C(31)−Zr(1)−N(1) 76.0(4).

resonances of the silane products (Ph_2SiH_2, Ph_3SiH, and Ph_4Si), from which **7** could not be isolated cleanly. However, **7** can be prepared independently by the reaction of **6** with H_2, as shown in eq 4.

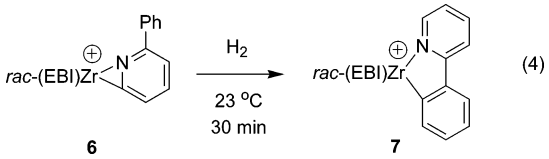

(4)

The molecular structure of **7** was established by X-ray diffraction and is shown in Figure 4. The 2-(2-pyridyl)-phenyl ligand is bonded in the plane between the two indenyl ligands in an η^2(*C*,*N*) fashion and forms a five-membered chelate ring. The angle between the phenyl and the pyridine ring planes is 7.5(1)°. The *rac*-(EBI)Zr framework adopts a conformation in which the indenyl C_6 rings project forward over the two "equatorial" coordination sites.[23]

Scheme 12

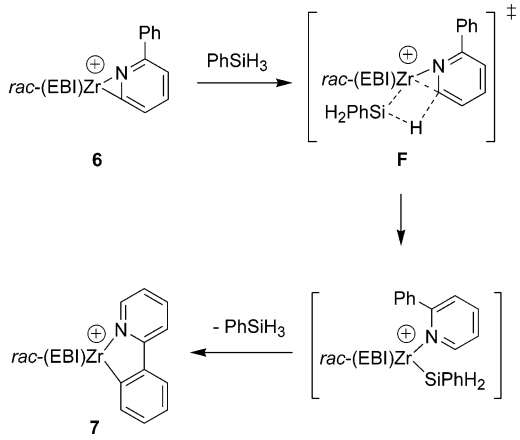

The NMR spectra of **7** are fully consistent with the solid state structure. The number, intensities, and multiplicities of the ^{1}H NMR aromatic resonances, and the ^{1}H−^{1}H COSY spectrum, establish that **7** contains two inequivalent indenyl ligands, an ortho-disubstituted phenyl ring, and an ortho-substituted pyridine ring, which is consistent with metalation of an ortho-phenyl position of the phenylpyridine unit. The Zr−$C_{Ph,ipso}$ ^{13}C resonance appears at δ 193.3, close to that for $Cp_2ZrPh(THF)^+$ (δ 184.9).[18] The ortho-pyridine ^{1}H NMR resonance of **7** (H21 in Figure 4) was assigned on the basis of NOESY data and a deuterium labeling experiment (**6** + D_2) and appears at δ 6.03, far upfield of the corresponding resonance of free 2-Ph-pyridine (δ 8.59), due to anisotropic shielding by the proximate indenyl C_6 ring. This result establishes that the pyridine is N-coordinated to Zr. Similarly, the ortho-phenyl resonance (H30 in Figure 4) is shifted upfield to δ 5.84.

Mechanism of Formation of 7. The $PhSiH_3$-mediated isomerization of **6** to **7** likely proceeds by the mechanism in Scheme 12. Complex **6** and $PhSiH_3$ react via σ-bond metathesis transition state **F**, in which Si occupies a position α to Zr, to yield *rac*-(EBI)Zr($SiPhH_2$)-(2-Ph-pyridine)$^+$. It is not known if the N-coordination is retained in **F**. Subsequent remote C−H activation yields **7** and regenerates $PhSiH_3$. The reaction of **2** with 0.2 equiv of $PhSiH_3$ (85 °C, 22 h) produces **7** in 90% yield, which confirms that the conversion of **6** to **7** is catalytic in $PhSiH_3$. The H_2-mediated isomerization of **6** to **7** proceeds by an analogous mechanism.[24]

The remote C−H activation to form a five-membered metallacycle in Scheme 12 is unusual for zirconocene systems,[2] but common for group 7−10 metal systems.[25] For example, $MeMn(CO)_5$ reacts with 2-phenylpyridine to yield $Mn(CO)_4${η^2(*C*,*N*)-2-(2-pyridyl)phenyl}.[25c,26]

Reaction of [Cp_2Zr{η^2(*C*,*N*)-CH_2CHMe(6-methyl-2-pyridyl)}][$B(C_6F_5)_4$] (3) with $PhSiH_3$. The reaction

(19) For examples of samarium-mediated activations of Si−aryl bonds, see: (a) Castillo, I.; Tilley, T. D. *J. Am. Chem. Soc.* **2001**, *123*, 10526. (b) Castillo, I.; Tilley, T. D. *Organometallics* **2000**, *19*, 4733. (c) Radu, N. S.; Hollander, F. J.; Tilley, T. D.; Rheingold, A. L. *J. Chem. Soc., Chem. Comm.* **1996**, 2459.

(20) The presence of $(C_5R_5)_2ZrPh^+$, other minor $(C_5R_5)_2Zr$ species, and the silane products in the $(C_5R_5)_2ZrH^+$ oils formed in the reactions of **1a**,**b** with $PhSiH_3$ explains why these oils solidify much more slowly than those generated by reaction of **1a**,**b** with H_2. The slower oil solidification in the $PhSiH_3$ reactions explains why more extensive reaction with the chlorobenzene solvent occurs.

(21) $[Ph_3C][B(C_6F_5)_4]$ is known to mediate organosilane redistribution reactions (see refs 3d and 22). Since $[Ph_3C][B(C_6F_5)_4]$ is used to generate **1a**,**b**, it is possible that trace $[Ph_3C][B(C_6F_5)_4]$ could play a role in the observed silane redistribution chemistry. To ensure that no $[Ph_3C][B(C_6F_5)_4]$ was present, Cp_2ZrMe_2 was reacted with 0.9 equiv of $[Ph_3C][B(C_6F_5)_4]$ to produce a mixture of **1a** and [{Cp_2ZrMe}$_2$(μ-Me)]-$[B(C_6F_5)_4]$. This solution, free of Ph_3C^+, reacted with 1 equiv of $PhSiH_3$ to form the same silane products as observed when **1a** was generated from 1:1 mixtures of Cp_2ZrMe_2 and $[Ph_3C][B(C_6F_5)_4]$. Additionally, ^{19}F NMR studies show that extensive anion degradation occurs in the reaction of $[Ph_3C][B(C_6F_5)_4]$ with $PhSiH_3$. In contrast, no anion degradation is observed in the reaction of **1a**,**b** with $PhSiH_3$. Therefore, we conclude that trace $[Ph_3C][B(C_6F_5)_4]$ is not responsible for the silane redistribution observed in the reaction of **1a**,**b** with $PhSiH_3$.

(22) Corey, J. Y. *J. Am. Chem. Soc.* **1975**, *97*, 3227.

(23) (a) Jordan, R. F.; LaPointe, R. E.; Baenziger, N.; Hinch, G. D. *Organometallics* **1990**, *9*, 1539. (b) Schafer, A. K.; Zsolnai, L.; Huttner, G.; Brintzinger, H. H. *J. Organomet. Chem.* **1987**, *328*, 87.

(24) It is also possible that a trace amount of H_2 is formed in the reactions of **2** and **6** with $PhSiH_3$ and catalyzes the conversion of **6** to **7**.

(25) (a) Newkome, G. R.; Puckett, W. E.; Gupta, V. K.; Kiefer, G. E.; *Chem. Rev.* **1988**, *86*, 451. (b) Omae, I. *Chem. Rev.* **1979**, *79*, 287. (c) Bruce, M. I.; Goodall, B. L.; Matsuda, I. *Aust. J. Chem.* **1975**, *28*, 1259.

(26) The observed isomerization of **6** to **7** in the presence of H_2 (eq 4) or $PhSiH_3$ (Schemes 11 and 12) implies that **7** is more stable than **6**. Therefore, the formation of **6** in the reaction of *rac*-(EBI)ZrMe-$(ClC_6D_5)^+$ and 2-phenylpyridine (Scheme 4) and the general preference for the formation of η^2-pyridyl products in related C−H activations (ref 2) must result from kinetic control.

Scheme 13

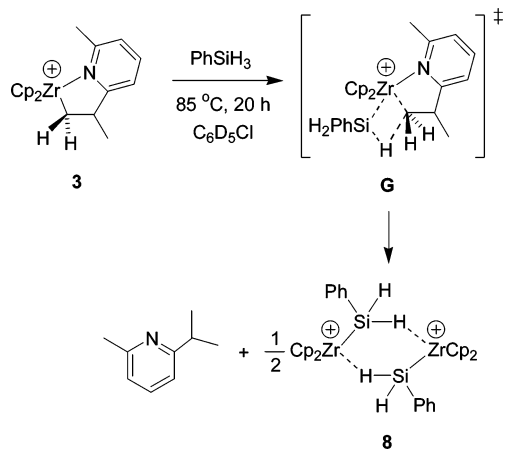

Scheme 14

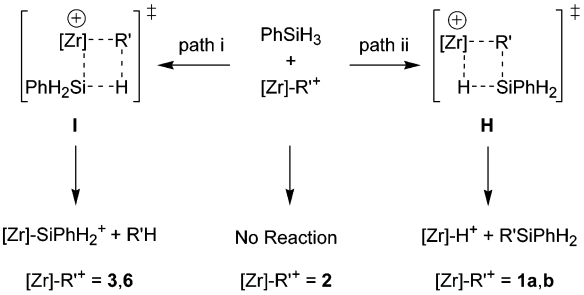

of **3** with 2 equiv of $PhSiH_3$ at 85 °C in C_6D_5Cl results in complete consumption of **3** and consumption of 1 equiv of $PhSiH_3$. One major organometallic product (>90% yield) is observed and was identified as $[\{Cp_2ZrSiPhH_2\}_2][B(C_6F_5)_4]_2$ (**8**) by ^1H, ^{19}F, ^{29}Si, and NOESY NMR data, which are in close agreement with data for the corresponding $BBu_n(C_6F_5)_{4-n}^-$ ($n = 0, 1, 2$) salt reported by Harrod.[4b] One equivalent of 2-Me-6-^{i}Pr-pyridine is formed per Cp_2Zr unit of **8**.[27] These results are consistent with a σ-bond metathesis reaction between **3** and $PhSiH_3$ via transition state **G** in Scheme 13, in which Si occupies the position α to Zr. It is not known if the N-coordination is retained in **G**.

Discussion

The primary goal of this work is to probe the feasibility of harnessing σ-bond metathesis reactions of silanes to convert $(C_5R_5)_2Zr\{\eta^2(C,N)\text{-}CH_2CHR^1(6\text{-}R^2\text{-}2\text{-pyridyl})\}^+$ azazirconacycles to $(C_5R_5)_2ZrH^+$ and silyl-functionalized disubstituted pyridines, as shown in Scheme 2. As shown in Scheme 14, Zr-R′/Si−H σ-bond metathesis reactions can proceed by two pathways, which differ in the position of Si in the transition state (α or β to Zr). To achieve the desired "silanolytic" cleavage of Zr−C bonds in the azazirconacycles, it is required that the Zr−C/Si−H σ-bond metathesis proceed by path ii and transition state **H** in Scheme 14. The cationic Zr−Me species **1a**,**b** do indeed react with $PhSiH_3$ by path ii to generate $(C_5R_5)_2ZrH^+$ and $PhMeSiH_2$ as the initial products. However, the azazirconacycle **3** reacts with $PhSiH_3$ with opposite selectivity by path i to afford $(C_5R_5)_2ZrSiPhH_2^+$ and 2-Me-6-^{i}Pr-pyridine. A reasonable explanation for this difference in selectivity is that steric crowding imposed by the bulky pyridyl-alkyl unit in **3** disfavors transition state **H** in this case. The more crowded azazirconacycle species **2** does not react directly with $PhSiH_3$. In this case, deinsertion of propene occurs at elevated temperature to afford **6**, which is catalytically isomerized to **7** by $PhSiH_3$. The key step in this isomerization is Zr−C/Si−H σ-bond metathesis via path i. Steric crowding between the 6-phenyl-2-pyridyl ligand of **6** and the $-SiPhH_2$ group may disfavor transition state **H** in this case as well. However, further studies will be required to fully understand the selectivity in these reactions.

Conclusions

The $(C_5R_5)_2ZrR'^+$ cations **1a**,**b**, **3**, and **6** react with $PhSiH_3$ via σ-bond metathesis. The formation of $(C_5R_5)_2ZrH^+$ and $R'SiH_2Ph$ as initial products in the reaction of **1a**,**b** demonstrates that σ-bond metathesis with silanes is a *potentially* viable pathway for Zr−C bond cleavage and functionalization of $(C_5R_5)_2ZrR'^+$ species. However, several issues must be addressed in order to exploit this chemistry for the functionalization of the azazirconacycle intermediates in catalytic olefin-pyridine coupling processes, including (i) tuning the $(C_5R_5)_2ZrR'^+$ and silane steric properties to favor the desired selectivity (path ii in Scheme 14), (ii) avoiding the photochemical reaction of $(C_5R_5)_2ZrH^+$ species with chlorinated solvents, and (iii) preventing dimerization and concomitant deactivation of the $(C_5R_5)_2ZrH^+$ species.

Experimental Section

General Procedures. All manipulations were performed under purified N_2 or vacuum using standard Schlenk techniques or in a nitrogen-filled drybox unless otherwise noted. Nitrogen was purified by passage through columns of activated molecular sieves and Q-5 oxygen scavenger. Benzene and hexanes were purified by passage through columns of activated alumina and BASF R3-11 oxygen removal catalyst. C_6D_5Cl and C_6H_5Cl were distilled from P_2O_5 and stored under vacuum prior to use. THF-d_8 was purchased from Cambridge Isotopes and dried over Na/benzophenone and stored under vacuum prior to use. CD_3CN was purchased from Cambridge Isotopes and dried and stored over 4 Å molecular sieves under vacuum prior to use. $[Ph_3C][B(C_6F_5)_4]$ was obtained from Boulder Scientific and used as received. 2-Phenylpyridine, 2-picoline, $PhSiH_3$, Me_3SiCl, Ph_3CCl, D_2, and propene were purchased from Aldrich and used as received. Hydrogen was purchased from Airco and used as received. Cp_2ZrMe_2 (Cp = C_5H_5),[28a] Cp'_2ZrMe_2 (Cp′ = C_5H_4Me),[28b] and *rac*-(EBI)$ZrMe_2$ (EBI = 1,2-ethylene-bis-indenyl)[28c] were prepared by literature procedures. $[Cp_2ZrMe(ClPh)][B(C_6D_5)_4]$ (**1a**) and $[Cp'_2ZrMe(ClPh)][B(C_6D_5)_4]$ (**1b**) were generated as described elsewhere.[8] Elemental analyses were performed by Midwest Microlabs (Indianapolis, IN). GC-MS analyses were performed on a HP-6890 instrument equipped with a HP-5973 mass selective detector. Infrared spectra were recorded on a Nicolet NEXUS

(27) Me-6-^{i}Pr-pyridine is observed in the GC-MS of the reaction mixture. However, the ^1H NMR resonances for 2-Me-6-^{i}Pr-pyridine in the reaction mixture are shifted slightly upfield from the free substrate positions, which is attributed to interaction of the pyridine with trace zirconium species in the mixture. Isolated samples of **8** always contain a trace amount of 2-Me-6-^{i}Pr-pyridine.

(28) (a) Samuel, E.; Rausch, M. D. *J. Am. Chem. Soc.* **1973**, *95*, 6263. (b) Couturier, S.; Tainturier, G.; Gautheron, B. *J. Organomet. Chem.* **1980**, *195*, 291. (c) Diamond, G. M.; Peterson, J. L.; Jordan, R. F. *J. Am. Chem. Soc.* **1996**, *118*, 8024.

470 FT-IR spectrometer. ESI-MS experiments were performed with a HP Series 1100MSD instrument using direct injection via a syringe pump (ca. 10^{-6} M solutions). Good agreement between observed and calculated isotope patterns was observed, and the listed *m/z* value corresponds to the most intense peak in the isotope pattern.

NMR spectra were recorded in sealed tubes on Bruker AMX-400 or AMX-500 spectrometers at ambient temperature unless otherwise indicated. ^{1}H and ^{13}C chemical shifts are reported versus Me_4Si and were determined by reference to the residual solvent peaks. ^{11}B, ^{19}F, and ^{29}Si chemical shifts were referenced to external neat $BF_3{\cdot}Et_2O$, neat $CFCl_3$, and neat Me_4Si, respectively. Coupling constants are reported in Hz. Quantitative ^{1}H NMR measurements were performed using Cp_2Fe as an internal standard.

^{13}C, ^{19}F, and ^{11}B NMR spectra of ionic compounds contain $B(C_6F_5)_4^-$ resonances at the free anion positions. $^{13}C\{^1H\}$ NMR (C_6D_5Cl): δ 148.9 (dm, $J = 240$, C2), 138.7 (dm, $J = 230$, C4), 136.8 (dm, $J = 238$, C3), 124.4 (br, C1). ^{19}F NMR (C_6D_5Cl): δ −130.2 (br s, 2F, F_o), −160.3 (t, $J = 23$, 1F, F_p), −164.3 (t, $J = 19$, 2F, F_m). ^{11}B NMR (C_6D_5Cl): δ −15.8 (br s).

NMR spectra of in-situ generated $(C_5R_5)_2ZrMe(ClC_6D_5)^+$ species **1a**,**b** contain resonances for Ph_3CMe. NMR data for Ph_3CMe: ^{1}H NMR (C_6D_5Cl): δ 7.14−7.05 (m, 15H, Ph), 2.03 (s, 3H, Me). $^{13}C\{^1H\}$ NMR (C_6D_5Cl): δ 149.4 (ipso Ph), 129.0 (Ph), 128.1 (Ph), 126.2 (Ph), 52.8 (C), 30.6 (Me).

[*rac*-(EBI)Zr{η^2(*C*,*N*)-CH_2CHMe(6-phenyl-2-pyridyl)}][$B(C_6F_5)_4$] (2). This species was prepared previously as the $MeB(C_6F_5)_3^-$ salt.[2a] A flask was charged with *rac*-(EBI)$ZrMe_2$ (0.380 g, 1.08 mmol) and $[Ph_3C][B(C_6F_5)_4]$ (1.00 g, 1.08 mmol). A solution of 2-phenylpyridine (0.160 mL, 1.09 mmol) in C_6H_5Cl (20 mL) was added by cannula. The mixture was vigorously stirred for 2 h at 23 °C. The flask was cooled to −196 °C, and propene (10.8 mmol, 10 equiv) was added by vacuum transfer. The flask was warmed to 23 °C and vigorously stirred overnight, resulting in a dark yellow solution. The volatiles were removed under vacuum to yield a dark yellow oil. The oil was washed with benzene (3 × 10 mL) and dried under vacuum overnight to afford pure **2** as a dark yellow solid (0.95 g, 85%). ^{1}H NMR (C_6D_5Cl): δ 7.70 (d, $J = 9$, 1H, indenyl C_6), 7.50 (m, 2H, Ph), 6.60 (d, $J = 3$, 1H, indenyl C_5), 6.39 (d, $J = 9$, 1H, indenyl C_6), 5.74 (d, $J = 3$, 1H, indenyl C_5), 5.56 (br, 2H, Ph), 5.37 (d, $J = 3$, 1H, indenyl C_5), 3.33 (d, $J = 3$, 1H, indenyl C_5), 3.33 (m, 1H, CH_2CH_2), 3.18 (m, 1H, CH_2CH_2), 3.07 (m, 1H, CH_2CH_2), 2.91 (m, 2H, CH_2CH_2 and $-CH_2CHMe$), 1.02 (d, $J = 5$, 3H, $-CH_2CHMe$), 0.36 (dd, $J = 10$, 5; 1H, $-CH_2CHMe$), −1.31 (t, $J = 10$, 1H, $-CH_2CHMe$). The other indenyl C_6, phenyl, and pyridyl resonances are masked by the solvent resonances.

[Cp_2Zr{η^2(*C*,*N*)-CH_2CHMe(6-methyl-2-pyridyl)}][$B(C_6F_5)_4$] (3). This species was prepared previously as BPh_4^- salt.[2h] A flask was charged with Cp_2ZrMe_2 (0.902 g, 3.59 mmol) and $[Ph_3C][B(C_6F_5)_4]$ (3.29 g, 3.57 mmol), and 2-methylpyridine (0.750 mL, 7.60 mmol) and C_6H_5Cl (60 mL) were added. The mixture was vigorously stirred for 1 h at 23 °C. The flask was cooled to −196 °C, and propene (28.7 mmol, ca. 8 equiv) was added by vacuum transfer. The flask was warmed to 23 °C and vigorously stirred overnight, resulting in a dark yellow solution. The volatiles were removed under vacuum to yield a dark brown oil. The oil was washed with benzene (3 × 10 mL) and dried under vacuum overnight to afford pure **3** as a dark yellow solid (3.69 g, 95%). ^{1}H NMR (C_6D_5Cl): δ 7.31 (t, $J = 8$, 1H, py), 6.81 (d, $J = 8$, 1H, py), 6.57 (d, $J = 8$, 1H, py), 5.97 (s, 5H, Cp), 5.96 (s, 5H, Cp), 3.13 (m, 1H, $-CH_2CHMe$), 2.46 (dd, $J = 6$, 5; 1H, $-CH_2CHMe$), 1.10 (d, $J = 6$, 3H, $-CH_2CHMe$), 1.09 (s, 3H, py *Me*), 0.41 (dd, $J = 6$, 5; 1H, $-CH_2CHMe$).

Reaction of [$Cp_2ZrMe(ClC_6D_5)$][$B(C_6F_5)_4$] (1a) with $PhSiH_3$ in C_6D_5Cl. A solution of **1a** (0.048 mmol) and Ph_3CMe (0.048 mmol) in C_6D_5Cl (0.5 mL) was prepared in an NMR tube, and $PhSiH_3$ (6.0 μL, 0.048 mmol) was added by microsyringe. The tube was maintained at 23 °C *under ambient room light* and vigorously agitated. A dark red solution formed immediately, and a dark red oil separated at the bottom of the NMR tube within 20 min. The oil solidified to form an orange crystalline solid within 6 days at 23 °C. The volatiles were vacuum-transferred into another NMR tube containing Cp_2Fe as an internal standard. NMR analysis established that C_6D_5H (δ 7.21, s, 0.012 mmol) was the major species present and that trace amounts of Ph_2SiH_2, SiH_4, and CH_4 were also present. The presence of C_6D_5H was confirmed by GC-MS analysis (*m/z* = 83 (M^+)).

C_6D_5Cl (0.5 mL) was added to the residue remaining after the removal of the volatiles from the reaction tube to afford a slurry of an orange precipitate in a dark red supernatant. The supernatant was decanted away from the precipitate. A portion of the supernatant (0.2 mL) was diluted with benzene (1 mL) and analyzed by GC-MS, which established that the following compounds were present (*m/z* values of M^+ ions are given in parentheses): $PhSiMeH_2$ (122), $PhSiMe_2H$ (136), $PhSiMe_3$ (150), Ph_2SiH_2 (184), Ph_2SiMeH (198), Ph_2SiMe_2 (212), Ph_3SiH (260), Ph_3SiMe (274), Ph_4Si (336), and $C_6D_5-C_6D_5$ (164). No other Si-containing species were detected by GC-MS.

The orange precipitate from above was washed with benzene (3 × 1 mL) and dried under vacuum overnight to afford an orange solid. The solid was dissolved in THF-d_8 at −90 °C to yield a yellow solution, which was maintained and analyzed by ^{1}H NMR at −90 °C. The ^{1}H NMR spectrum contained resonances at δ 6.98 and 6.75 in an 1:3 intensity ratio, corresponding to $[\{Cp_2Zr(\mu\text{-}Cl)\}_2][B(C_6F_5)_4]_2$ (**4a**) and $[\{Cp_2Zr(\mu\text{-}H)\}_2][B(C_6F_5)_4]_2$ (**5a**). In a similar experiment under identical conditions, the yields of **4a** and **5a** were determined to be 23% and 72%, respectively, versus starting **1a**, based on integration of the Cp resonances versus the Ph_3CMe resonance. Additionally, single crystals of **4a** were selected from the orange solid under a microscope and characterized by X-ray diffraction.

In a series of similar experiments *under ambient room light*, the organometallic products were analyzed at different stages of the oil solidification process. These results reveal that the ratio of **4a/5a** increases with time as described in the text. Additionally, the reaction of **1a** with $PhSiH_3$ was conducted under similar conditions *in the dark*. ^{1}H NMR analysis showed that **5a** was formed in greater than 90% yield and **4a** was not formed.

Reaction of [$Cp'_2ZrMe(ClC_6D_5)$][$B(C_6F_5)_4$] (1b) with $PhSiH_3$ in Chlorobenzene. The reaction of **1b** (0.041 mmol) with $PhSiH_3$ (5.0 μL, 0.041 mmol) in C_6D_5Cl (0.5 mL) *under ambient room light* was studied, and the products were analyzed using the procedures described above for **1a**. These analyses showed that the reaction of **1b** with $PhSiH_3$ afforded C_6D_5H, $[\{Cp'_2Zr(\mu\text{-}Cl)\}_2][B(C_6F_5)_4]_2$ (**4b**), and $[\{Cp'_2Zr(\mu\text{-}H)\}_2][B(C_6F_5)_4]_2$ (**5b**) in a 2:1:2 molar ratio. The organic products, identified by GC-MS, include $PhSiMeH_2$, $PhSiMe_2H$, $PhSiMe_3$, Ph_2SiH_2, Ph_2SiMeH, Ph_2SiMe_2, Ph_3SiH, Ph_3SiMe, Ph_4Si, and $C_6D_5-C_6D_5$. Similarly, the reaction of **1b** (0.060 mmol) with $PhSiH_3$ (7.5 μL, 0.060 mmol) in C_6H_5Cl (0.5 mL) was conducted *in the dark*, and the products were analyzed using the procedures described above for **1a**. These analyses showed that **5b** was formed in >90% yield and **4b** was not formed.

[$\{Cp_2Zr(\mu\text{-}Cl)\}_2$][$B(C_6F_5)_4$]$_2$ (4a). Method 1: A solution of **1a** (0.039 mmol) in C_6D_5Cl (0.5 mL) was generated in a valved NMR tube and cooled to −196 °C. Me_3SiCl (0.041 mmol) was added by vacuum transfer. The tube was warmed to 23 °C and vigorously agitated. The tube was maintained at 23 °C overnight, and a suspension of a dark yellow precipitate in an orange supernatant formed. The supernatant was decanted away from the solid. The solid was washed with benzene (3 × 1 mL) and dried under vacuum overnight to afford **4a** as a dark yellow solid in ca. 80% yield. Method 2: A solution of **1a** (0.047 mmol) in C_6D_5Cl (0.5 mL) was prepared in a valved NMR tube, and Ph_3CCl (13 mg, 0.047 mmol) was added. The

tube was maintained at 23 °C and monitored periodically by NMR. After 2 days, the ^{1}H NMR resonances of **1a** had disappeared and orange crystals had formed. The crystals were collected, washed with benzene (3 × 1 mL), and dried under vacuum overnight to afford **4a** as a dark yellow solid in ca. 90% yield. An analytically pure sample of **4a** was obtained from method 1. Anal. Calcd: C, 43.63; H, 1.08. Found: C, 43.87; H, 1.46. ESI-MS (THF-d_8 solution): Major cation observed: $[\{Cp_2Zr(\mu\text{-}Cl)\}_2^{2+} - H^+ - 2H]$ calcd *m/z* 506.9, found 506.8.

NMR Analysis of [{Cp$_2$Zr(μ-Cl)}$_2$][B(C$_6$F$_5$)$_4$]$_2$ (4a). ^{1}H NMR (THF-d_8, −90 °C): δ 6.98 (s, 10H, Cp). ^{13}C NMR (THF-d_8, −90 °C): δ 119.7 (Cp). ^{1}H NMR (THF-d_8, 23 °C): δ 6.87 (s, 10H, Cp). ^{13}C NMR (THF-d_8, 23 °C): δ 119.8 (Cp). **4a** also dissolves in acetonitrile to form a mixture of $Cp_2ZrCl(NCCD_3)_n^+$, Cp_2ZrCl_2, and $Cp_2Zr(NCCD_3)_3^{2+}$. ^{1}H NMR (CD_3CN, −40 °C): δ 6.53 (s, Cp_2ZrCl_2), 6.49 (s, $Cp_2Zr(NCCD_3)_3^{2+}$), 6.38 (s, $Cp_2ZrCl(NCCD_3)_n^+$). ^{1}H NMR (CD_3CN): δ 6.52 (s, Cp_2ZrCl_2), 6.51 (s, $Cp_2Zr(NCCD_3)_3^{2+}$), 6.39 (s, $Cp_2ZrCl(NCCD_3)_n^+$).[29]

[{Cp′$_2$Zr(μ-Cl)}$_2$][B(C$_6$F$_5$)$_4$]$_2$ (4b). This complex was generated in 85% yield from **1b** (0.052 mmol) and Me_3SiCl (0.055 mmol) using method 1 described above for **4a**. ^{1}H NMR (THF-d_8, −90 °C): δ 6.89 (m, 4H, Cp′), 6.66 (m, 4H, Cp′), 2.26 (s, 6H, Cp′*Me*). ^{13}C NMR (THF-d_8, −90 °C): δ 128.0 (Cp′ ipso), 118.8 (Cp′), 117.4 (Cp′), 15.8 (Cp′*Me*). ^{1}H NMR (THF-d_8, 23 °C): δ 6.76 (m, 4H, Cp′), 6.56 (m, 4H, Cp′), 2.29 (s, 6H, Cp′*Me*). ^{13}C NMR (THF-d_8, 23 °C): δ 128.9 (Cp′ ipso), 119.7 (Cp′), 117.1 (Cp′), 16.1 (Cp′*Me*).[29]

[{Cp$_2$Zr(μ-H)}$_2$][B(C$_6$F$_5$)$_4$]$_2$ (5a). An amberized NMR tube containing a solution of **1a** (0.043 mmol) in C_6D_5Cl (0.5 mL) was immersed in liquid nitrogen and exposed to H_2 (600 Torr, ca. 0.065 mmol). The tube was sealed, warmed to 23 °C, and vigorously agitated, resulting in a suspension of a yellow solid in an orange supernatant. The tube was maintained at 23 °C in the dark. A ^{1}H NMR spectrum was recorded after 10 min and showed that **1a** had reacted completely. The volatiles were removed under vacuum. The residue was washed with benzene (3 × 1 mL) and dried under vacuum to afford **5a** as a yellow solid in 95% yield. Anal. Calcd: C, 45.30; H, 1.23. Found: C, 45.41; H, 1.59. IR (**5a**, Nujol): ν_{Zr-H} = 1337 cm^{-1}. [{Cp$_2$Zr(μ-D)}$_2$][B(C$_6$F$_5$)$_4$]$_2$ (**5a**-d_2) was generated from **1a** and D_2 using the procedure for **5a**. IR (**5a**-d_2, Nujol): ν_{Zr-D} = 1040 cm^{-1}.

NMR Analysis of [{Cp$_2$Zr(μ-H)}$_2$][B(C$_6$F$_5$)$_4$]$_2$ (5a). ^{1}H NMR (THF-d_8, −90 °C): δ 6.75 (s, 20H, Cp), −0.53 (s, 2H, μ-H). ^{13}C NMR (THF-d_8, −90 °C): δ 113.1 (Cp). ^{1}H NMR (THF-d_8, 23 °C): δ 6.20 (s, 10H, Cp), 5.78 (s, 1H, Zr−H). ^{13}C NMR (THF-d_8, 23 °C): δ 108.5 (Cp). The dramatic shift of the hydride resonance between −90 and 23 °C is attributed to the formation of $Cp_2ZrH(THF\text{-}d_8)^+$. Complex **5a** is also soluble in CD_3CN, in which the insertion product $[Cp_2Zr(N\text{-}CHCD_3)(CD_3CN)][B(C_6F_5)_4]$ is formed.[14b] ^{1}H NMR (CD_3CN): δ 8.50 (br s, 1H, N-C*H*CD$_3$), 6.25 (s, 10H, Cp).

[{Cp′$_2$Zr(μ-H)}$_2$][B(C$_6$F$_5$)$_4$]$_2$ (5b). This complex was generated in 95% yield from **1b** (0.049 mmol) and H_2 (0.065 mmol) using the procedure for **5a**. **5b** is soluble in THF due to the formation of $[Cp'_2ZrH(THF\text{-}d_8)][B(C_6F_5)_4]$. ^{1}H NMR (THF-$d_8$, −40 °C): δ 6.25 (m, 2H, Cp′), 6.20 (m, 2H, Cp′), 6.02 (m, 2H, Cp′), 5.89 (s, 1H, terminal Zr−H), 5.63 (m, 2H, Cp′), 2.28 (s, 6H, Cp′*Me*). ^{1}H NMR (THF-d_8): δ 6.30−5.90 (br, 8H, Cp), 6.19 (br s, 1H, terminal Zr−H), 2.27 (s, 6H, Cp′*Me*). These data agree with values for the analogous BPh_4^- salt.[14a]

Generation of [*rac*-(EBI)Zr{η^2(*C,N*)-(6-phenyl-2-pyridyl)}][B(C$_6$F$_5$)$_4$] (6). This species was prepared previously as $MeB(C_6F_5)_3^-$ salt.[2a] An NMR tube was charged with *rac*-(EBI)$ZrMe_2$ (15.8 mg, 0.053 mmol), $[Ph_3C][B(C_6F_5)_4]$ (42.0 mg, 0.053 mmol), and 2-phenylpyridine (7.1 μL, 0.055 mmol). C_6D_5Cl (0.5 mL) was added by vacuum transfer at −196 °C. The tube was warmed to 23 °C and vigorously agitated, resulting in a dark orange solution. The tube was maintained at 23 °C for 2 h. A ^{1}H NMR spectrum was recorded and showed that **6** had formed quantitatively. ^{1}H NMR (C_6D_5Cl): δ 7.71 (d, J = 9, 1H, py), 6.87 (t, J = 8, 1H, indenyl C$_6$), 6.74 (d, J = 8, 1H, indenyl C$_6$), 6.47 (t, J = 8, 1H, indenyl C$_6$), 6.17 (d, J = 8, 1H, indenyl C$_6$), 6.07 (d, J = 3, 1H, indenyl C$_5$), 5.90 (d, J = 3, 1H, indenyl C$_5$), 5.01 (d, J = 3, 1H, indenyl C$_5$), 4.95 (d, J = 3, 1H, indenyl C$_5$), 3.50−3.12 (m, 4H, CH_2CH_2). The other indenyl C$_6$, phenyl, and pyridyl signals were masked by resonances from the solvent and Ph_3CMe.

[*rac*-(EBI)Zr{η^2(*C,N*)-2-(2-pyridyl)phenyl}][B(C$_6$F$_5$)$_4$] (7). Complex **7** was generated by three methods. Method 1: A solution of **2** (20.5 mg, 0.017 mmol) in C_6D_5Cl (0.5 mL) was prepared in an NMR tube. $PhSiH_3$ (5.4 μL, 0.043 mmol) was added by microsyringe. The tube was vigorously agitated, resulting in a yellow solution. The tube was maintained at 23 °C and monitored periodically by NMR. No reaction was observed after 10 h. The tube was maintained at 85 °C for 20 h. The color of the solution changed to dark red, and ^{1}H NMR analysis showed that **2** was completely consumed and **7** had formed quantitatively. Additionally, $PhSiH_3$ (0.017 mmol), Ph_2SiH_2 (0.012 mmol), and a trace amount of SiH_4 were observed by ^{1}H NMR analysis, and their quantities were determined by integration versus the $-CH_2CH_2-$ resonances of **7**. The volatiles were removed under vacuum. The residue was washed with C_6D_6 (1 mL) and dried under vacuum to afford **7** as a red solid in 90% purity. The ^{1}H NMR spectrum of the C_6D_6 wash contained characteristic resonances for atactic oligopropene. ^{1}H NMR (C_6D_6): δ 1.65 (br, −C*H*), 1.35−0.81 (br, CH_2 and −Me).[30] GC-MS analysis of the C_6D_6 wash showed that Ph_3SiH and Ph_4Si were present. Method 2: A solution of **6** (0.054 mmol) in C_6D_5Cl (0.5 mL) at 23 °C was generated in an NMR tube as described above, and $PhSiH_3$ (7.0 μL, 0.056 mmol) was added by microsyringe. The tube was vigorously agitated, resulting in a red solution. The tube was maintained at 23 °C for 30 min. ^{1}H NMR analysis showed that **6** was completely consumed. The volatiles were removed under vacuum. The residue was washed with benzene (3 × 1 mL) and dried under vacuum to afford **7** as a red solid in 90% purity. Method 3: An NMR tube containing a solution of **6** (0.046 mmol) in C_6D_5Cl (0.5 mL) was immersed in liquid nitrogen and exposed to H_2 (600 Torr, ca. 0.065 mmol). The tube was sealed, warmed to 23 °C, and vigorously agitated, resulting in a red solution. The tube was maintained at 23 °C for 30 min. ^{1}H NMR analysis showed that **6** was completely consumed. The volatiles were removed under vacuum. The residue was washed with benzene (3 × 1 mL) and dried under vacuum to afford **7** as an analytically pure, red solid in 95% yield. Anal. Calcd: C, 55.94; H, 2.05; N, 1.19. Found: C, 56.27; H, 1.79; N, 1.38.

NMR Data for [*rac*-(EBI)Zr{η^2(*C,N*)-2-(2-pyridyl)-phenyl}][B(C$_6$F$_5$)$_4$] (7). The numbering system for **7** is shown in Figure 4. ^{1}H NMR (C_6D_5Cl): δ 7.41 (m, 1H, H23), 7.39 (d, J = 8, 1H, H24), 7.32 (d, J = 8, 1H, H27), 7.20 (d, J = 8, 1H, indenyl C$_6$), 7.05 (d, J = 8, 1H, indenyl C$_6$), 6.99 (m, 1H, H28), 6.94 (m, 1H, indenyl C$_6$), 6.92 (m, 1H, H29), 6.84 (t, J = 8, 1H, indenyl C$_6$), 6.68 (m, 1H, H22), 6.66 (d, J = 8, 1H, indenyl C$_6$), 6.58 (d, J = 3, 1H, indenyl C$_5$), 6.38 (m, 2H, indenyl C$_6$), 6.25 (t, J = 8, 1H, indenyl C$_6$), 6.23 (d, J = 3, 1H, indenyl C$_5$), 6.03 (d, J = 6, 1H, H21), 5.92 (d, J = 3, 1H, indenyl C$_5$), 5.84 (d, J = 8, 1H, H30), 5.77 (d, J = 3, 1H, indenyl C$_5$), 3.75 (m,

(29) The ^{1}H and ^{13}C NMR spectra of THF-d_8 solutions of **4a**,**b** at −90 °C show that these species have C_{2v} symmetry. This is consistent with dinuclear Zr(μ-Cl)$_2$Zr structures, as observed in the solid state, or mononuclear $(C_5R_5)_2ZrCl(THF\text{-}d_8)^+$ adducts that undergo rapid intermolecular THF-d_8 exchange with accompanying site epimerization at Zr, or rapid dimer/monomer equilibria. ESI-MS results for **4a**, and the absence of line broadening of the Cp′ ^{1}H and ^{13}C NMR resonances of **4b** at −90 °C, suggest that these species retain their dinuclear structures in THF-d_8 solution.

(30) Stockland, R. A.; Foley, S. R.; Jordan, R. F. *J. Am. Chem. Soc.* **2003**, *125*, 796.

Table 1. Summary of X-ray Diffraction Data for 4a, 4b, and 7

	$[\{Cp_2Zr(\mu\text{-}Cl)\}_2][B(C_6F_5)_4]_2$ (**4a**)	$[Cp'_2Zr(\mu\text{-}Cl)\}_2][B(C_6F_5)_4]_2$ (**4b**) + 2 C_6D_5Cl	[*rac*-(EBI)Zr{η^2-(*C,N*)-2-(2-pyridyl)-phenyl}][$B(C_6F_5)_4$] (**7**)
formula	$C_{68}H_{20}B_2Cl_2F_{40}Zr_2$	$C_{84}H_{28}D_{10}B_2Cl_4F_{40}Zr_2$	$C_{55}H_{24}BF_{20}NZr$
fw	1871.80	2163.10	1180.78
cryst syst	triclinic	triclinic	monoclinic
space group	$P\bar{1}$	$P\bar{1}$	$P2_1/c$
a (Å)	10.006(2)	11.684(2)	27.854(6)
b (Å)	12.497(3)	13.503(3)	18.962(4)
c (Å)	13.971(3)	13.712(3)	17.008(3)
α (deg)	64.50(1)	85.33(1)	
β (deg)	87.26(1)	68.09(1)	91.45(3)
γ (deg)	84.66(1)	75.77(1)	
V (Å^3)	1570(1)	1945(1)	8980(3)
Z	2	2	8
T (K)	100	100	100
cryst color, habit	red, fragment	red, fragment	red-orange, plate
GOF on F^2	1.063	0.982	1.342
R indices ($I > 2\sigma(I)$)[a]	R1 = 0.0378	R1 = 0.0579	R1 = 0.0942
	wR2 = 0.0943	wR2 = 0.1507	wR2 = 0.1706
R indices (all data)[a]	R1 = 0.0417	R1 = 0.0681	R1 = 0.1009
	wR2 = 0.0969	wR2 = 0.1589	wR2 = 0.1737

[a] $R1 = \sum||F_o| - |F_c||/\sum|F_o|$; $wR2 = [\sum[w(F_o^2 - F_c^2)^2]/\sum[w(F_o^2)^2]]^{1/2}$, where $w = q[\sigma^2(F_o^2) + (aP)^2 + bP]^{-1}$.

1H, CH_2CH_2), 3.47 (m, 1H, CH_2CH_2), 3.27 (m, 2H, CH_2CH_2). ^{13}C NMR (C_6D_5Cl): δ 193.3 (C31), 160.7 (C25), 145.5 (C21), 141.9 (C24), 139.2 (C26), 137.4 (C30), 130.9 (C29), 130.1 (ipso indenyl), 129.4 (indenyl C_6), 129.0 (indenyl C_6), 128.0 (C28), 127.1 (ipso indenyl), 126.4 (ipso indenyl), 126.2 (indenyl C_6), 126.1 (indenyl C_6), 125.4 (indenyl C_6), 125.0 (indenyl C_6), 124.8 (ipso indenyl), 124.0 (C27), 123.1 (ipso indenyl), 122.3 (C22), 121.4 (ipso indenyl), 121.1 (indenyl C_6), 119.8 (C23), 119.7 (indenyl C_6), 116.4 (indenyl C_5), 116.3 (indenyl C_5), 112.6 (indenyl C_5), 110.5 (indenyl C_5), 28.8 (CH_2CH_2), 28.3 (CH_2CH_2). The ^1H NMR assignments were confirmed by $^1H-^1H$ COSY and NOESY NMR. The ^{13}C NMR assignments were established by $^1H-^{13}C$ HMQC NMR.

Generation of [{$Cp_2Zr(SiH_2Ph)$}$_2$][$B(C_6F_5)_4$]$_2$ (8). A solution of **3** (23.8 mg, 0.024 mmol) in C_6D_5Cl (0.5 mL) was prepared in an NMR tube, and $PhSiH_3$ (5.6 μL, 0.045 mmol) was added by microsyringe at 23 °C. The tube was vigorously agitated, resulting in a yellow solution. The tube was maintained at 85 °C for 20 h. The color of the solution changed to orange, and ^1H NMR analysis showed that complete consumption of **3** and 50% consumption of $PhSiH_3$ had occurred, **8** had formed in ca. 90% yield, and 1 equiv of 2-Me-6-^{i}Pr-pyridine had formed per $Cp_2ZrSiH_2Ph^+$ unit of **8**.[24] Less than 10% of unidentified impurities were also present. The volatiles were vacuum transferred into another NMR tube. ^1H NMR analysis of the volatiles showed that 2-Me-6-^{i}Pr-pyridine was present. ^1H NMR (2-Me-6-^{i}Pr-pyridine, C_6D_5Cl): δ 7.23 (t, J = 8, 1H, py), 6.76 (d, J = 8, 1H, py), 6.70 (d, J = 8, 1H, py), 2.98 (septet, J = 6, 1H, C*H*Me$_2$), 2.38 (s, 3H, py *Me*), 1.23 (d, J = 6, 6H, CH*Me*$_2$). GC-MS analysis of the volatiles confirmed the presence of 2-Me-6-^{i}Pr-pyridine (m/z = 135 (M^+)). The residue was washed with benzene (3 × 1 mL) and dried under vacuum to afford **8** as a yellow solid in 80% yield. **8** was identified by comparison of the ^1H, ^{29}Si, and NOESY NMR data for **8** with reported data for the corresponding $BBu_n(C_6F_5)_{4-n}^-$ (n = 0, 1, 2) salt.[4] Data for [{$Cp_2Zr(SiH_2Ph)$}$_2$][$B(C_6F_5)_4$]$_2$ (**8**): ^1H NMR (C_6D_5Cl): δ 7.68 (d, J = 8, 2H, Ph), 7.28 (m, 1H, Ph), 6.97 (m, 2H, Ph), 5.95 (s, 1H, Si−H), 5.42 (s, 5H, Cp), 5.34 (s, 5H, Cp), −3.15 (s, 1H, μ Si−H). ^1H NMR (C_6D_6): δ 7.56 (m, 2H, Ph), 7.30 (m, 1H, Ph), 7.00 (m, 2H, Ph), 5.80 (s, 1H, Si−H), 5.13 (s, 5H, Cp), 5.06 (s, 5H, Cp), −3.38 (s, 1H, μ Si−H). ^{29}Si NMR (C_6D_5Cl): δ 105. Key $^1H-^1H$ NOESY correlations δ/δ: 7.68 (Ph)/-3.15 (μ Si−H); 5.95 (Si−H)/-3.15 (μ Si−H); 5.42 (Cp)/-3.15 (μ Si−H); 5.34 (Cp)/-3.15 (μ Si−H).

X-ray Crystallography. Crystallographic data are summarized in Table 1. Full details are provided in the Supporting Information. Data were collected on a Bruker Smart Apex diffractometer using Mo Kα radiation (0.71073 Å). Nonhydrogen atoms were refined with anisotropic displacement coefficients. All hydrogen atoms were included in the structure factor calculation at idealized positions and were allowed to ride on the neighboring atoms with relative isotropic displacement coefficients. ORTEP diagrams are drawn with 50% probability ellipsoids. Specific comments for each structure are as follows. **4a**: Single crystals of **4a** were obtained from the reaction of **1a** with Ph_3CCl in C_6D_5Cl at 23 °C. **4b**: Single crystals of **4b** were obtained from the reaction of **1b** with $PhSiH_3$ in C_6D_5Cl under ambient room light at 23 °C. The asymmetric unit contains one solvent molecule (C_6D_5Cl). **7**: Single crystals of **7** were obtained by slow diffusion of hexanes into a concentrated C_6D_5Cl solution of **7** (generated by method 3 described above) at 23 °C. The asymmetric unit contains two independent molecules of **7**, whose structures are very similar.

Acknowledgment. This work was supported by the National Science Foundation (CHE-0212210). We thank Edward J. Stoebenau, III for helpful discussions and Dr. Ian Steele for the X-ray diffraction analyses.

Supporting Information Available: Tables of X-ray crystallographic data, atomic coordinates, bond lengths and bond angles, and anisotropic thermal parameters for **4a**, **4b**, and **7** (PDF and CIF files). This material is available free of charge via the Internet at http://pubs.acs.org.

OM049099Z